Antarctic Science 17 (4): 541–553 (2005) © Antarctic Science Ltd Printed in the UK DOI: 10.1017/S0954102005002968

Antarctic glacial isostatic adjustment: a new assessment

ERIK R. IVINS[1]* and THOMAS S. JAMES[2]

[1]*Jet Propulsion Laboratory, California Institute of Technology, Pasadena, CA 91109, USA*
[2]*Geological Survey of Canada, Sidney, British Columbia V8L 4B2 Canada*
**eri@fryxell.jpl.nasa.gov*

Abstract: The prediction of crustal motions and gravity change driven by glacial isostatic adjustment (GIA) in Antarctica is critically dependent on the reconstruction of the configuration and thickness of the ice sheet during the Late Pleistocene and Holocene. The collection and analysis of field data to improve the reconstruction has occurred at an accelerated pace during the past decade. At the same time, space-based imaging and altimetry, combined with on-ice velocity measurements using Global Positioning System (GPS) geodesy, has provided better assessments of the present-day mass balance of the Antarctic ice sheet. Present-day mass change appears to be dominated by deglaciation that is, in large part, a continuation of late-Holocene evolution. Here a new ice load model is constructed, based on a synthesis of the current constraints on past ice history and present-day mass balance. The load is used to predict GIA crustal motion and geoid change. Compared to existing glacioisostatic models, the new ice history model is significantly improved in four aspects: (i) the timing of volume losses in the region ranging from the Ross Sea sector to the Antarctic Peninsula, (ii) the maximum ice heights in parts of the Ellsworth and Transantarctic Mountains, (iii) maximum grounding line position in Pine Island Bay, the Antarctic Peninsula, and in the Ross Sea, (iv) incorporation of present-day net mass balance estimates. The predicted present-day GIA uplift rates peak at 14–18 mm yr^{-1} and geoid rates peak at 4–5 mm yr^{-1} for two contrasting viscosity models. If the asthenosphere underlying West Antarctica has a low viscosity then the predictions could change substantially due to the extreme sensitivity to recent (past two millennia) ice mass variability. Future observations of crustal motion and gravity change will substantially improve the understanding of sub-Antarctic lithospheric and mantle rheology.

Received 14 January 2005, accepted 1 July 2005

Key words: Antarctica, glacial isostasy, global geodesy, GRACE satellites, mantle viscosity

Introduction

Glaciologists and glacial geologists are in general agreement that a more extensive Antarctic continental ice cover existed at Last Glacial Maximum (LGM) (~21 kyr BP) and that its size can be assessed. Constraints on ice mass changes during the Holocene and Late Pleistocene have been determined from glaciomarine sediments, volcanic marker horizons, surface exposure dating, inferences from radio echo sounding, ice flow modelling, ice core inferences of palaeoclimate, emergence of Holocene beaches, and analysis of lacustrine palaeoenvironments. These data are synthesized here to provide an improved glacial history. Our goal is to reduce the uncertainties in the forward modelling of relative sea-level and the geodetic quantities associated with glacial isostatic adjustment (GIA), including time-dependent gravity.

Early reconstructions of Antarctic ice sheet evolution produced a contribution to eustatic sea-level rise (ESLR), $\Delta\xi$ of 24–37 m, which was needed to explain the magnitude of observed far-field relative sea-level curves. Now, observations such as surface exposure dates of past ice sheet elevations (e.g. Ackert *et al*. 1999, Stone *et al*. 2003), and marine cores that establish the maximum grounding line positions of the LGM ice sheet (Bentley & Anderson 1998, Lowe & Anderson 2002, Anderson *et al.* 2002), directly constrain Antarctic ice sheet evolution. The main implication of the new constraints is the smaller values, by factors of 2 to 3, of Antarctic meltwater compared to the ICE-3G (Tushingham & Peltier 1991), ANT (Nakada & Lambeck 1988, 1989) and D91 (James & Ivins 1998) models. The D91 model (James & Ivins 1998) incorporated regional constraints (Denton *et al.* 1991, 1992, Licht *et al.* 1996), but these were sparse, both in space and in time, relative to the model presented here. Instead of $\Delta\xi$ ~24–37 m, more recent models provide 6–14 m (Bentley 1999, Denton & Hughes 2002), a reduction in the maximum contribution to sea-level of at least 60% from the earlier models. The recent glaciological models of Huybrechts (2002, 2004) also adhere to some of these new constraints.

Unlike the centres of glacioisostatic uplift in Fennoscandia and Canada, Antarctic crustal rebound remains poorly constrained due to a scarcity of near-field relative sea-level data. One of the main goals of temporal gravity satellite missions is to construct maps of the ongoing isostatic rebound in Antarctica, which will help to address the paucity of sea-level observations. The mapping has another application, as more reliable maps help disentangle the geodetic signals associated with present-day ice mass change from those linked to the major phase of deglaciation (Wahr *et al.* 2000, Wu *et al*. 2002). This paper offers maps of the predicted vertical bedrock velocity generated with a better-constrained evolution of the Antarctic ice sheet over the past 21 kyr. The results are relevant to ongoing GPS-based observations of neotectonics (e.g. Hothem *et al.* 2001, Negusini *et al*. 2005) and for all scientific problems in which the motion of Antarctic bedrock is relevant.

New ice load model: IJ05

We discuss the constraints in the western part of the Ross Sea sector and then move counter clockwise through the Antarctic sectors, from Victoria Land, to Dronning Maud Land, then across the Weddell Sea to the Antarctic Peninsula, and finally return to the central portion of the Ross Sea. Other recent reviews include Ingólfsson & Hjort (1999), Bentley (1999), Anderson *et al.* (2002), Huybrechts (2004) and Ingólfsson *et al.* (2003). The division of sectors follows Denton & Hughes (2002) (fig. 5, therein), and we term the new model 'IJ05'. The revised load model presented here is smaller than that of Denton & Hughes (2002), though we initially employed their model as a guide. Denton & Hughes' (2002) model is a descendent of the model of Denton *et al.* (1991) which we formerly gridded as 'D91' in James & Ivins (1998) and subsequently modified to D91-1.5 in Ivins *et al*. (2001).

Tables I and II give the volumes and eustatic sea-level rise (ESLR) values for each of the Antarctic sectors at LGM and

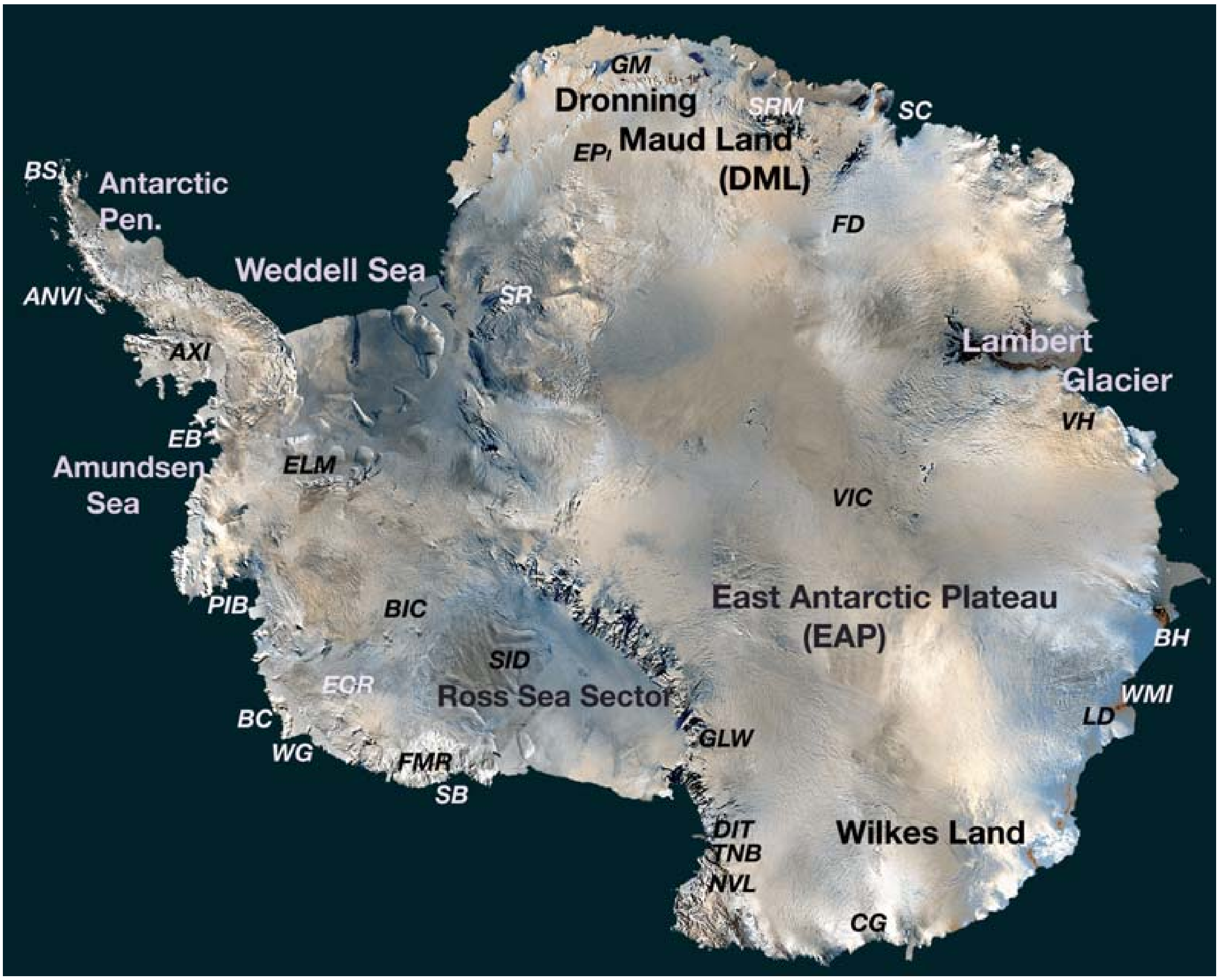

Fig. 1. United States Geological Survey Antarctic composite relief map with locations. ANVI = Anvers Island, AXI = Alexander Island, BC = Bakutis Coast, BH = Bunger Hills, BIC = Byrd Ice Core, BS = Bransfield Strait, CG = Cape Gray, DIT = Drygalski Ice Tongue, EB = Eltanin Bay, ECR = Executive Committee Range, ELM = Ellsworth Mountains, EPI = EPICA Ice Core site, FD = Fuji Dome, FMR = Ford Mountain Ranges, GM = Gruber Mountains, GLW = Glacial Lake Wright, LD = Law Dome, NVL = North Victoria Land, PIB = Pine Island Bay, SB = Sulzberger Bay, SC = Syowa Coast, SID = Siple Ice Dome, SR = Shackleton Range, SRM = Sør Rondane Mountains, TNB = Terra Nova Bay, VH = Vestfold Hills, VIC = Vostok Ice Core, WG = Wrigley Gulf, WMI = Wind Mill Islands. Marguerite Bay is located just north of AXI.

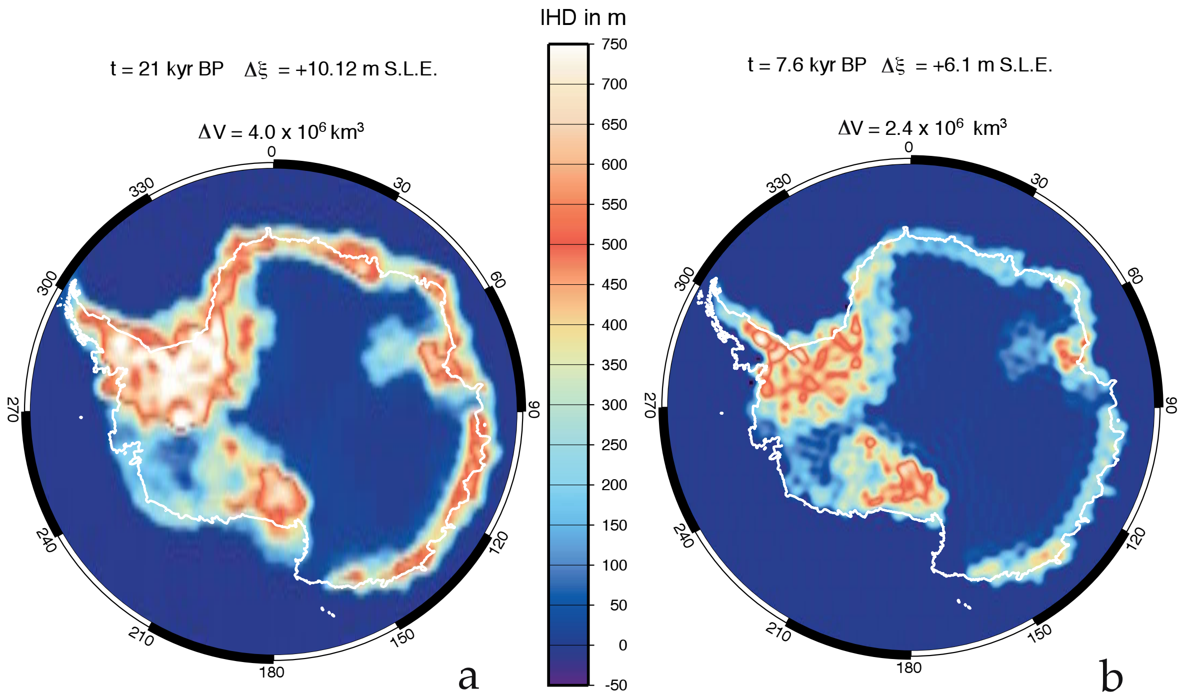

Fig. 2. Ice height differences (IHD) for the 'IJ05' ice history model at **a.** LGM at 21 kyr, and at **b.** 7.6 kyr BP. The differential ice height assumes zero values at present-day (modelled as AD 2000) and at 102 kyr BP. These maps are constructed via a disk representation (James & Ivins 1998, Ivins *et al*. 2003) and expanded in spherical harmonics with truncation at degree and order 256.

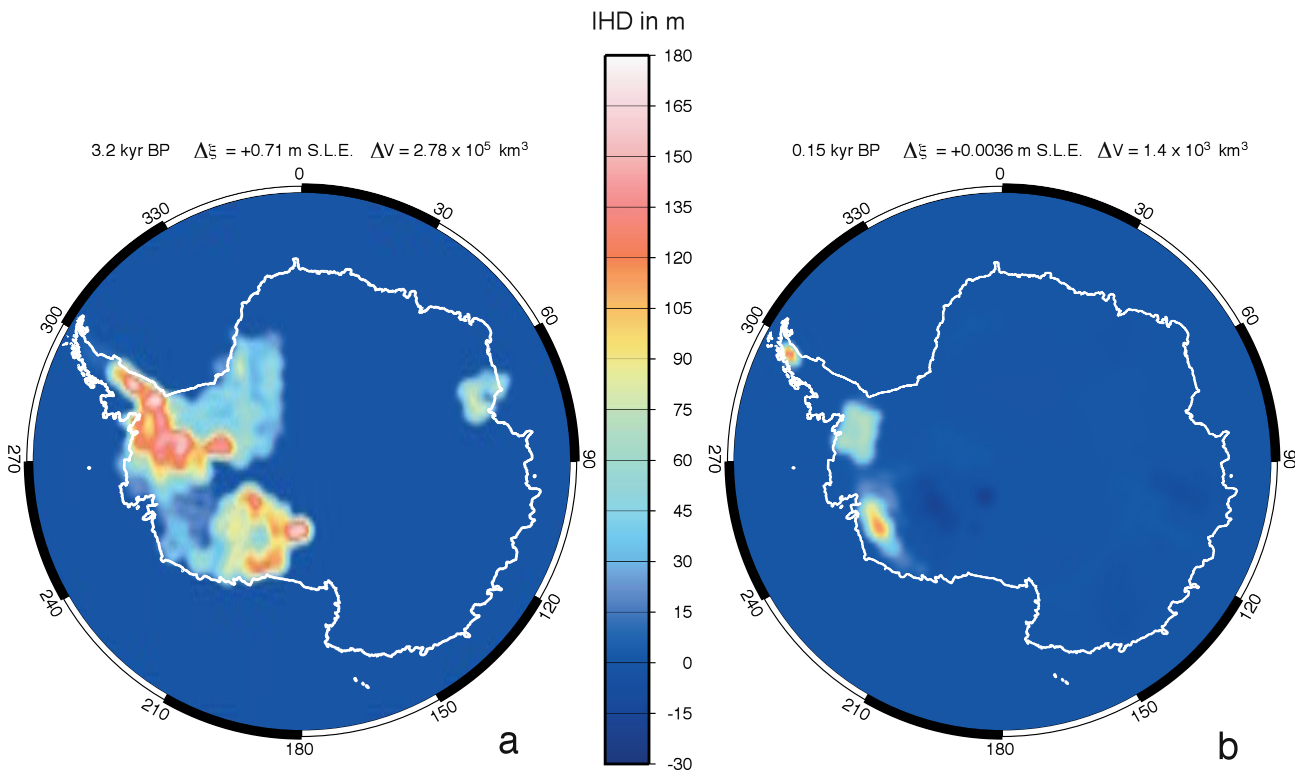

Fig. 3. Same as Fig. 2, but for ice height differences (IHD) at **a.** 3.2 kyr, and at **b.** 0.15 kyr BP. The negative heights in (b) indicate mass increase.

Table I. Last Glacial Maximum (21 kyr BP) load.

Region	ΔV (10^5 km^3)	Δξ (m)	Area (10^6 km^2)
Antarctic Peninsula	4.297	1.10	1.11
Amundsen Sea Sector	2.156	0.55	1.14
Weddell Sea Sector	10.280	2.63	1.94
Dronning Maud Land	6.587	1.69	1.47
Ross Sea Sector	5.071	1.30	1.84
Wilkes Land	5.774	1.48	1.94
Lambert Glacier	1.513	0.39	0.33
East Antarctic Plateau	3.847	0.99	7.44
Total	39.53	10.12	16.8

Table II. Mid-Holocene grounded ice.

Region t = 6.8 kyr BP	ΔV (km^3)	Δξ (m)
Antarctic Peninsula	2.62 x 10^5	0.67
Amundsen Sea Sector	0.90 x 10^5	0.23
Weddell Sea Sector	4.06 x 10^5	1.04
Dronning Maud Land	1.11 x 10^5	0.28
Ross Sea Sector	2.59 x 10^5	0.66
Wilkes Land	2.30 x 10^5	0.59
Lambert Glacier	0.96 x 10^5	0.25
East Antarctic Plateau	0.58 x 10^5	0.15
Total	1.52 x 10^6	3.95

Table III. Grounded volume of deglaciating ice (10^5 km^3).

	Time (kyr BP)					
Region	15	11.5	7.6	6.8	3.2	0.15
Wilkes Land	4.62	4.14	3.26	2.30	0.00	0.00
Lambert	1.45	1.21	1.12	0.96	0.18	0.02
DML	6.08	4.90	3.29	1.11	0.00	0.00
Weddell	11.95	8.01	6.41	4.06	1.08	0.09
Antarctic Peninsula	5.16	3.84	2.45	2.62	0.46	0.05
Amundsen	2.59	1.37	1.10	0.90	0.25	0.04
Ross Sector	6.76	5.29	4.18	2.59	0.72	0.08
EAP	3.85	3.78	3.26	2.30	0.00	0.00
Total	42.97	32.98	23.91	15.42	2.78	0.28

at 6.8 kyr BP, respectively. Table III gives the volumes for each sector at each time specified in the ice load model after LGM. Figure 2 shows the ice height differences (IHD; differences are relative to present day) at 21 kyr and at 7.6 kyr BP throughout Antarctica. Figure 3a shows the IHDs at 3.2 kyr and Fig. 3b shows the IHDs for the final past time t_{N-1}, which is poorly constrained, but which is assumed to be 0.15 kyr BP in Table III and Fig. 3b. The effect of varying this parameter is discussed in the section on uplift predictions.

Transantarctic Mountains and the Western Ross Sector

Models of the Ross Sea have been largely based upon moraine data and marine records seaward of the present-day Ross Ice Shelf. Dating the deposits and ice polished rock surfaces has been a major challenge. Radiocarbon dating of material on raised beaches along coastal South Victoria Land at Dunlop Island (~77°S, 200 km south of the DIT, see Fig. 1) suggests higher ice elevations of about 500 m at 11–13 kyr BP (Hall *et al.* 2004). Ice height differences recorded in the adjacent Transantarctic Mountain Ranges (TAM) require the past ice sheet elevations to diminish with distance along a south-to-north trend, with IHD ~500 m higher at GLW (Hall *et al*. 2001), to less than 100–200 m just north-west of TNB during the past 21 kyr BP (Oberholzer *et al.* 2003). Along the margins of the TAM in NVL, the East Antarctic Ice Sheet appears to have had minimal expansion during and after LGM. In the revised load history, IHD values do not exceed 75 m just north of GLW and thin progressively to 20 m in NVL. Shipp *et al.* (1999) show that the grounding line position at LGM was south of the northernmost extent of NVL in the western Ross Sea.

Reduced ocean-continent moisture flux at LGM appears to characterize all of the EAP (East Antarctic Plateau). Numerical simulations of LGM climate by Toracinta *et al.* (2004) suggests that the zonally-averaged mean precipitation may have been reduced by a factor of two south of 70°S. At LGM the interior of the Antarctic continent was relatively precipitation starved. The retreat in the Ross Sea follows from a recent chronology developed by Licht (2004).

Wilkes Land to Dronning Maud Land

Wilkes Land, with its vast coastline east of NVL extending from 150 to 80°E, has sparse field constraints. However, new developments have emerged since the publication of the D91-1.5 model (Ivins *et al.* 2001). Several key features come from three distinct regions having ice-free exposure at present-day where moraine and lacustrine deposits have been dated. The transition from marine to lacustrine environments in the VH indicates that regional unloading was complete by about 11–9.5 kyr BP (Zwartz *et al.* 1998). However, also adjacent to Prydz Bay, near the Lambert Glacier, the Larsemann Hills appear to have been deglaciated by 13.5 kyr BP (Verleyen *et al.* 2004). In the BH and in the WMI, 1200 km to the east, emergence records indicate that deglaciation was complete by 9.5 kyr BP (Gore *et al.* 2001). Although it is difficult to estimate palaeotopography of the ice sheet here, IHD estimates range from 200 to 1000 m for coastal Wilkes Land (Bentley 1999). Ice core data from LD (van Ommen *et al.* 2004) suggest that LGM ice was ~150–250 m thicker than at present. This is a four-fold decrease in the IHD values that were assumed by the D91-1.5 model. These changes in the load model have very important implications for the GIA crustal response.

Our revised model has maximum IHD values near 650 m at LGM. These reduce to 250–475 m by 15 kyr BP, with the coastline becoming ice-free by 11.5 kyr BP. Interior IHD values are 100 to 300 m from 11.5 to 7.6 kyr BP, consistent with ice core indicators of increased storminess (Lorius *et al.* 1985, van Ommen *et al.* 2004) and interpretation of RSL data (Verleyen *et al.* 2005). A substantial improvement of the updated load model is the refinement of the grid structure, which allows offshore and coastal retreat, while permitting IHD values to also be specified 50–200 km inland. A more accurate portrayal of the inference by Domack *et al.* (1991) of a mid-Holocene readvance near CG (Fig. 1) is captured in the new grid-scheme. Constraints in the Lambert Glacier region are poor, and the reconstruction in our updated model reflects the values suggested in the numerical models of Huybrechts (2002) and Denton & Hughes (2002). Generally, the sector-by-sector LGM ΔV values (Table I) are similar to those reported by Denton & Hughes (2002) (identical sector boundaries are employed).

Ice core data from the 2.5 km deep drill hole at FD also provides new information as this core is located at the highest point in eastern Dronning Maud Land, at the north-eastern boundary of the EAP. The surface palaeotemperature history reconstructed from the deep core is remarkably consistent with those derived from the VIC (Parrenin *et al.* 2004) located 1500 km further east in the EAP (Watanabe *et al.* 2003). This indicates that spatially homogeneous climatic conditions prevailed in the interior of East Antarctica throughout glacial times. The core data support the view of a precipitation-starved Antarctic interior at LGM (Lorius *et al.* 1985). Generally, the updated model presented here has IHD values in the EAP of no more than 20 m, a value small enough that it has negligible influence on the magnitude of present-day uplift predictions.

Radiocarbon-dated deposits along the SC yield minimum emergence times for the last interglacial (isotope stage 5) and the mid-Holocene (Miura *et al.* 1998, Takada *et al.* 2003). The shoreline emergence data was modelled by Nakada *et al.* (2000) with regional IHD values of about 200–500 m, thickening from offshore to continent. A numerical reconstruction of Huybrechts (2002) has similar heights, but with thicker offshore ice. Our regional reconstruction is similar to that of Nakada *et al.* (2000). Further to the east, Pattyn & Decleir (1998) have modelled the ice sheet history near the SRM where exposure ages constrain LGM values of IHD. Between the coast and the SRM the IHD values at LGM are probably in the 20–400 m range (Pattyn & Decleir 1998, Huybrechts 2002). Our model tends to the high side of these values. In westernmost Dronning Maud Land dated lacustrine sediments and avian rookeries suggest IHD values as high as 900 m in the GM, but lower IHD values (~130 m) are inferred several hundred kilometres to the west (Scheinert *et al.* 2005). In the SR, at the western margins of Dronning Maud Land, surface exposure dates from glacially sculpted rock outcrops indicate IHD of less than 340 m (Fogwill *et al.* 2004).

Weddell Sea, Antarctic Peninsula and Amundsen Sea sectors

The Weddell Sea sector may have contained about one sixth of the total LGM mass in Antarctica that has contributed to postglacial sea-level rise (Denton & Hughes 2002). Reconstructions based upon sedimentary core data and bathymetric and seismic mapping suggest that the LGM grounding line was near the continental shelf (Anderson *et al.* 2002), at about the 500 m depth contour. Radiocarbon data from the eastern Weddell Sea suggest that deglaciation at the northernmost grounding line position was underway by 21 kyr BP (Bentley & Anderson 1998). On the western boundary of the Weddell Sea all chronological indicators suggest a prolonged period of deglaciation, extending into the mid-to-late Holocene (Hjort *et al*. 1997, Ivins *et al.* 2000, Ingólfsson *et al.* 2003). Analyses of ^{10}Be exposure dates in the southern ELM by Todd *et al.* (2004) indicate IHDs of about 430 to 1250 m. Deglaciation may have been a continuous process from about the time of the Antarctic Cold Reversal (ACR) (~13–14 kyr BP).

Ice grounded offshore of the Antarctic Peninsula occupied the BS to depths of at least 750 m at LGM (Bentley & Anderson 1998, Evans *et al.* 2004) where large ice streams carved a unique submarine glacial bathymetry (Canals *et al.* 2000). Radiocarbon dates obtained in the northern Peninsula indicate prolonged deglaciation, and a possible readvance in mid-Holocene times. Recent dating of isolation basins north of AXI by Bentley *et al.* (2005) indicate that the coastline of Marguerite Bay became ice free by 9 kyr BP. For comparison, the new IJ05 model has an IHD value of 188 m at 11.5 kyr, linearly decreasing to 0 m at 7.6 kyr BP. Although the model just north of AXI on the western margin of the Antarctic Peninsula has sufficient resolution for predicting present-day uplift and geoid rates of change, local refinements would be required to model relative sea-level changes.

Modelling by Payne *et al.* (1989) suggests an extensive ice sheet on the western margins of the Peninsula at LGM, including regions to the south-west (see EB in Fig. 1, also see Fig. 2). Ice covered most of ANVI and extended south to include AXI (Ingólfsson *et al.* 2003). To the west of EB in the Bellongshausen Sea, LGM ice was grounded near the continental shelf break (Hillenbrand *et al.* 2005). Further to the west in the Amundsen Sea Sector, data from multi-beam acoustic mapping reveal that ice sheet growth occurred in PIB, offshore of the BC and in the WG to about the 500 m contour on the continental shelf (Anderson & Shipp 2001, Anderson *et al.* 2002). Dated cores in PIB indicate that grounding line retreat was underway by 16 kyr BP and complete before 10 kyr BP (Lowe & Anderson 2002).

Western and Central Ross Sea sectors

Cowdery *et al.* (2004) reported that glaciers feeding into the

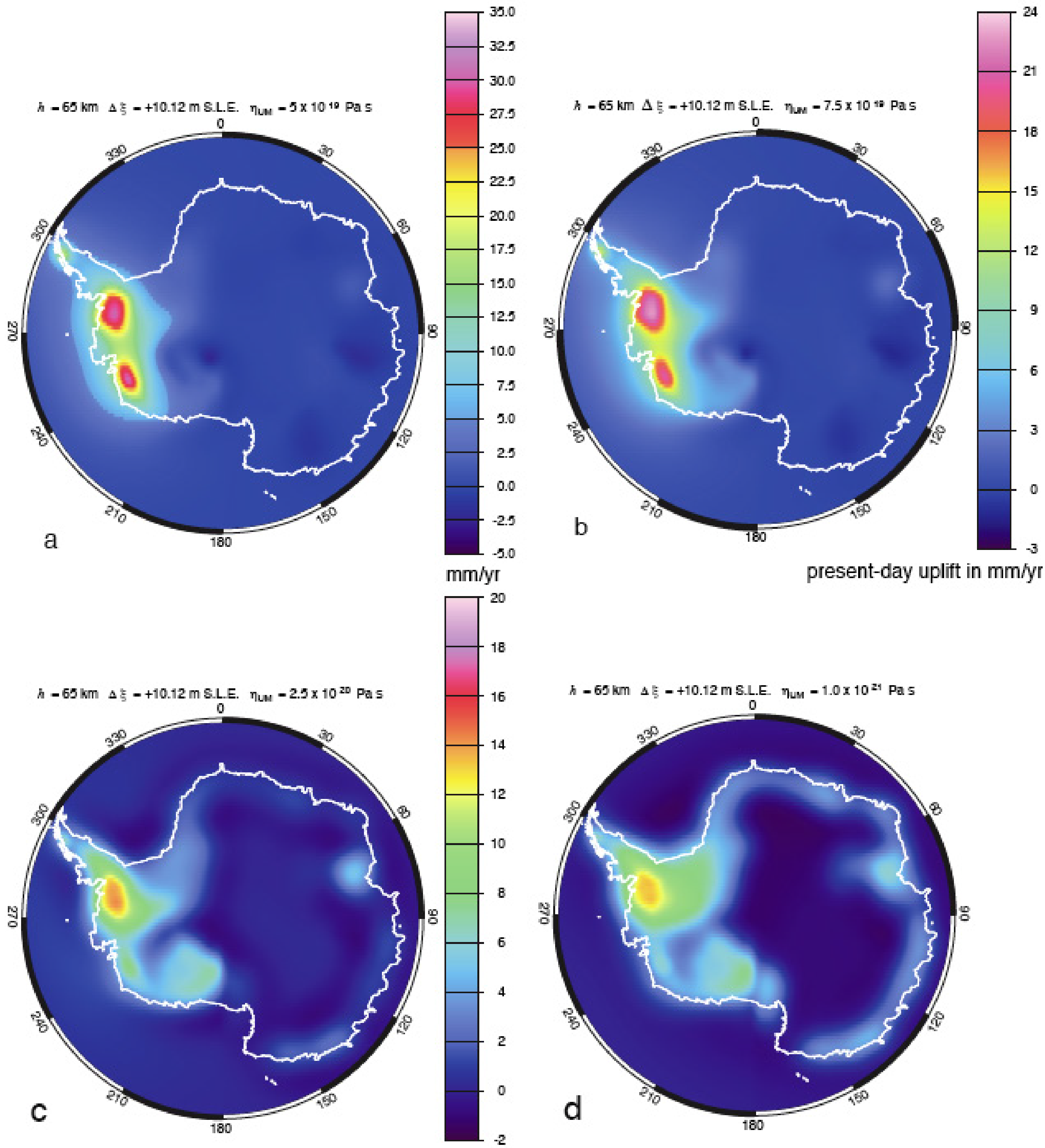

Fig. 4. Uplift rates (mm yr^{-1}) predicted for the IJ05 load model for four different mantle viscosity values using a half-space model. Here present-day ice changes are extrapolated back to 150 yr BP (t_{N-1}), and late Holocene change occurs from 3.2 kyr BP (t_{N-3}) to 800 yr BP (t_{N-2}). The pattern of uplift in frame **a.** is chiefly generated by late 20th century mass change (Rignot & Thomas 2002, Rignot *et al*. 2004a, 2004b). Frames **b.** to **d.** show the increasing influence of earlier ice change as viscosity is increased. An elastic lithosphere of thickness h = 65 km is assumed. Elastic rigidities are μ_{HS} = 145.0, μ_{lid} = 67.0 GPa and densities; ρ_{HS} = 3590.1 and, ρ_{lid} = 2280.0 kg m^{-3} for the half-space and lithosphere, respectively.

BC and WG from the FMR have retreated very slowly from about 11 to 2 kyr BP, with fresh rock exposure as young as 0.3 kyr BP. To the south in the ECR, dated volcanic deposits (Ackert *et. al* 1999) indicate IHD < 100 m at LGM. This reflects a substantial reduction (> 50%) in IHD values in comparison to the D91-1.5 model. Ice draining into SB, and into the eastern and central Ross Sea, has been depositing meltwater into the global oceans up to at least 2 kyr BP, and probably continuing to the present-day (Conway *et al.* 1999, Anderson & Shipp 2001, Bindschadler & Bentley 2002, Emslie *et al.* 2003, Stone *et al.* 2003, Licht 2004). James Fastook modelled this process and the numerical calculations are integrated into a deglaciation chronology constructed by Licht (2004). Licht's model has a total sea-level contribution from the total Ross Sector (including the eastern Ross Embayment) of $\Delta\xi$ = 3–6 m. Steig *et al.* (2001) suggest IHD values of 200 m at the BIC site. Consequently our regional ice load model is smaller than D91-1.5, having a total $\Delta\xi$ contribution since LGM of 1.3 m (Table I). The chronology for the sector is consistent with Conway *et al.* (1999), Hall *et al.* (2004) and Licht (2004). For the Ross Sector, our updated model volume is one-third of the LGM model of Denton & Hughes (2002). The updated model presented in Fig. 2 may be viewed as a maximum volume interpretation in the Central Ross Sea since an analysis of ice core data and internal layering at SID by Waddington *et al.* (2005) suggests that IHD values at LGM were less than 400 m.

Summary

Among the various sources for postglacial eustatic sea-level rise, the role of grounded ice in Antarctica has been most contentious. Estimates of the additional continental ice mass vary from 0 to 1.3 x 10^7 Gt*. As discussed by James & Ivins (1998), the Antarctic component of most global models is rooted in the CLIMAP reconstruction of Denton & Hughes (1981). An example is the 'ICE-3G'model constructed by Tushingham & Peltier (1991). Other models, including 'D91' of James & Ivins (1998) and the 'ANT1 to ANT4' models (Nakada & Lambeck 1988, Nakada *et al.* 2000), are also derivatives of the CLIMAP reconstruction. A main feature of each of these models is their substantial total meltwater input ($\Delta\xi$) to the global far-field sea-level rise after Last Glacial Maximum (LGM).

There are some striking contrasts between the new IJ05 model and globally based models in current use. For example, the ICE-5G model constructed by Peltier (2004) is about 65% larger by volume and has a collapse phase concentrated between 9 and 4 kyr BP, during which time the ESLR rate due to Antarctica is roughly 5.5 mm yr^{-1} for the first two thousand years of deglaciation, dropping to 2.1 mm yr^{-1} at 7–4 kyr BP. The largest loss rate for IJ05, in contrast, provides an ESLR rate during 11.5–7.6 kyr BP of 1.75 mm yr^{-1}, and drops by more that an order of magnitude after 3.2 kyr BP. The small amount of mass delivered to the oceans by IJ05 implies that other ice sheets models need to deliver more meltwater in order to satisfy far-field observations of sea-level. Our ice sheet collapse model does not have step-like jumps that deliver ~5–7 m of global eustatic sea-level change corresponding to meltwater pulses 1a or 1b near 14.3 and 11.3 kyr BP.

Accurate estimation of the total mass of the water locked into the Antarctic ice sheet during 21–0 kyr BP, and especially over the past 5 kyr, is crucial for the prediction of present-day GIA crustal motion. An upper bound on the mass loss is provided by a best-fit to global eustatic change over 0–5 kyr BP reported by Fleming *et al.* (1998) and Lambeck *et al.* (2004) and this constraint is explicitly applied to mass loss from Antarctica during this time in the new IJ05 model. In the following section predictions are given for the present-day time-dependent bedrock motions and external gravity change driven by the Earth's elastic and viscous-gravitational response to continent-wide glacial mass changes.

Predicted uplift rates

The new ice model predicts secular geoid rates sufficiently large to be observed in the analysis of the Gravity Recovery and Climate Experiment (GRACE) gravity data (Wahr *et al.* 2000, Kaufmann 2000, Ivins *et al.* 2001, Wu *et al.* 2002). Here, however, the crustal uplift predictions are emphasized since there are ongoing comparisons of predictions and GPS datasets as recently discussed by Dietrich *et al.* (2004), Donnellan & Luyendyk (2004), Raymond *et al.* (2004) and Willis *et al.* (2003).

In Fig. 4 the past final time t_{N-1} is assumed to be 0.15 kyr BP. Figure 5 examines the effect of changing the past final time. Ice thicknesses are assumed to change linearly in each time segment in the ice load model. Post-0.15 kyr evolution assumes mass imbalance estimates from Rignot & Thomas (2002), Rignot *et al*. (2004a, 2004b) and Thomas *et al*. (2004). The backward extrapolation of these late 20th century and early 21st century changes can be important to GIA uplift predictions.

Mantle viscosity and integration of present-day changes with 'IJ05'

Our estimate of the error in ice load history is that a one sigma level error is roughly at 50 to 100% for any given post-LGM time for ice differential thicknesses larger than about 500 m. As the past history now includes relatively robust constraints, it is important to test the sensitivity of the forward modelled uplift rates to variations in mantle

* 3.6 x 10^5 Gt is equivalent to a melt volume capable of raising sea level by 1 m.

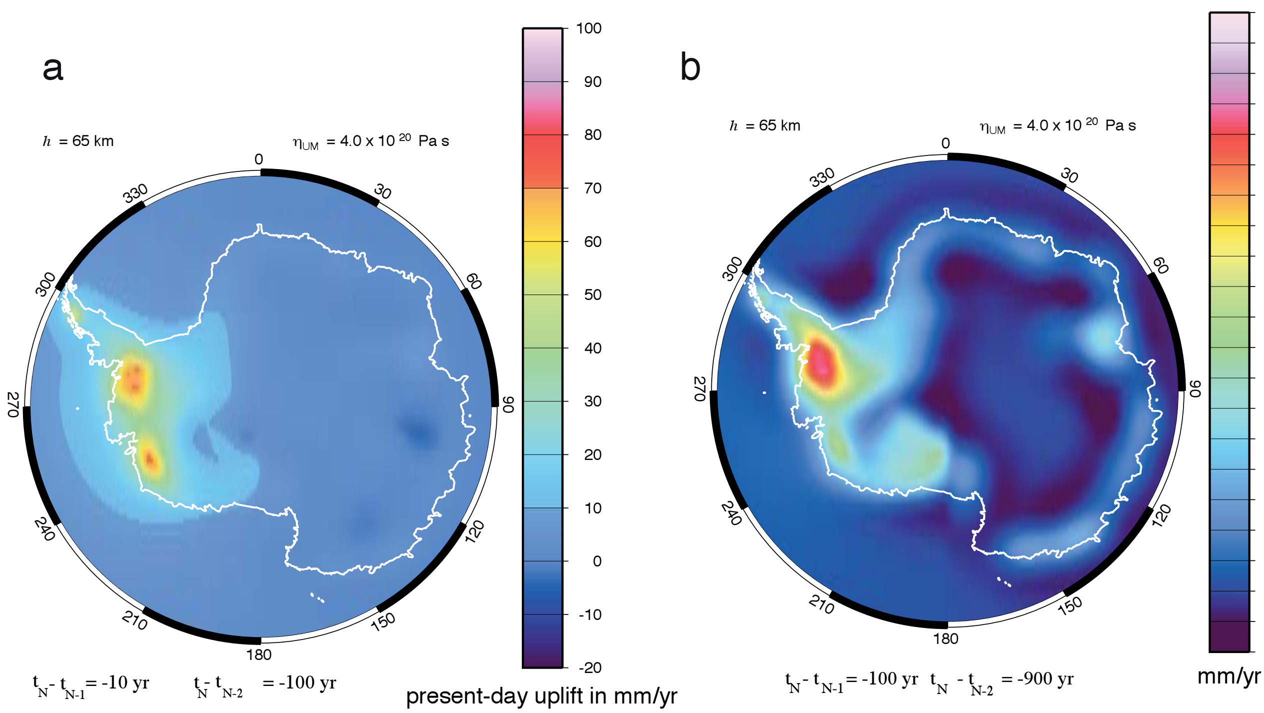

Fig. 5. Predicted uplift rates using the half-space model for two different load histories over the last millennium. Both frames **a.** & **b.** incorporate present-day changes, but (a) extrapolates present-day changes back to 10 yr BP, and assumes continuous late-Holocene change from 3.2 kyr to 100 yr. Frame (b) assumes backward extrapolation to 100 yr BP and steady Holocene rates from 3.2 kyr to 900 yr. Mantle viscosity is 4 x 10^{20} Pa s.

viscosity, and to the most recent ice-mass changes. The latter aspect remains troublesome. In Fig. 4 we conduct a simple experiment using a half-space model in which the viscosity increases from 5 x 10^{19} Pa s to 10^{21} Pa s, with all other Earth parameters and load history held constant. By using a half-space model we show the effects of the viscosity only. As the viscosity increases to 10^{21} Pa s, the late-Holocene and present-day changes become less important and memory of the LGM ice sheet becomes dominant. Preliminary estimates of lateral variations in viscosity by Kaufmann *et al.* (2005) span this viscosity range. Variations in seismic velocity in the uppermost mantle (e.g. Morelli & Danesi 2004) suggest that the spine of the TAM separates cold, sub-cratonic, mantle beneath East Antarctica from hotter mantle beneath West Antarctica. A recent analysis of satellite magnetic data from the Oersted and Challenging Minisatellite Payload (CHAMP) missions by Fox Maule *et al.* (2005) suggests relatively low crustal heat flux beneath the EAP. It is likely that the predictions with the smaller viscosity values are relevant to West Antarctica and the predictions with the larger viscosity values are relevant to East Antarctica (Kaufmann *et al.* 2005).

An aspect of the load history that is important for determining present-day crustal response rates is how the connection between present-day rates of ice-height change and Late Holocene ice-height change is made (Ivins *et al.* 2002). Present-day rates are based on observations from, at most, a few decades, and usually only a few years, whereas the constraints on Late Holocene ice-height changes may span a few thousand years. The rates of ice height change from the two time periods are generally different, and may even have the opposite sign. Consequently, it is necessary to decide how far back in time to extrapolate the present-day rates, t_{N-1}. Furthermore, the choice of an earlier model interface time, t_{N-2}, for the youngest age to which Holocene rates of ice mass change may be extrapolated, is also a sensitive and problematic model parameter. The choice of times t_{N-1} and t_{N-2} is important, as is shown in Fig. 5, as the extrapolation to 10 yr, and interface to 100 yr BP (frame a), has a factor of 5 larger predicted signal than does the case in frame (b), where extrapolation is to 100 yr and the interface is at 900 yr BP. The viscosity assumed in Fig. 5 (4 x 10^{20} Pa s) is consistent with the upper mantle derived from globally based models (Mitrovica & Forte 2004, Tosi *et al.* 2005). At a higher mantle viscosity (10^{21} Pa s), the interfacing and back-extrapolation is not as important because the earlier, larger ice-height changes dominate.

'Global Average' versus 'Stiff' sub-cratonic mantle viscosity

Here we employ a realistic, spherical, compressible Earth model with a moderate variability in mantle viscosity to predict uplift and geoid rates. The method of computation

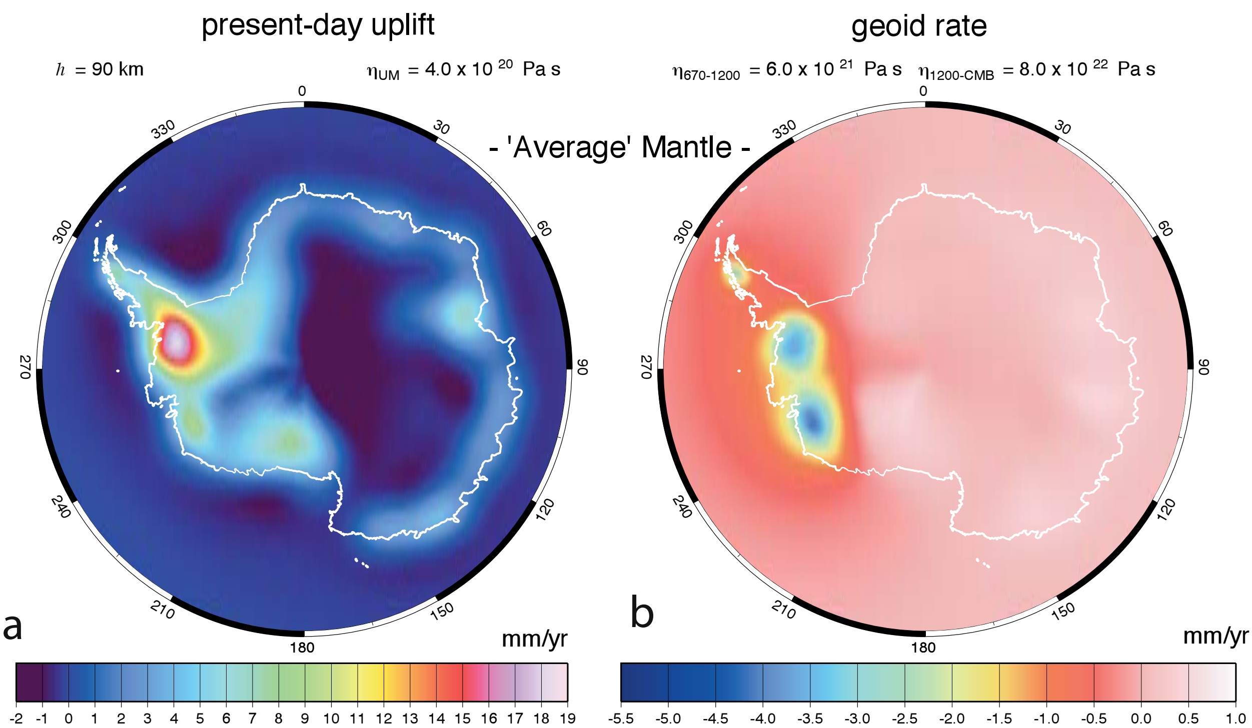

Fig. 6. a. Crustal uplift, and **b.** geoid rates predicted for the IJ05 model with the timing of the load as in Fig. 4. A compressible elastic lithosphere of thickness h = 90 km, a seismically realistic density profile, and a 3-layer viscosity structure is employed. The viscosity values (η) are for the upper mantle ('UM'), top of the lower mantle between 670 and 1200 km depth and bottom of the lower mantle between 1200 km depth and the core-mantle boundary (CMB). The radial viscosity profile is similar to a recent global estimate of Mitrovica & Forte (2004).

has been described by James & Ivins (1998) and the truncation is at degree 256. The past final time t_{N-1} is assumed to be 0.15 kyr BP, as in Fig. 4. Investigations of Laurentide and Fennoscandia GIA indicate that the upper mantle viscosity can be bounded to within a factor of 2–3 for these regions. Figure 4 clearly shows the important effects of a low viscosity ($\eta < 10^{20}$ Pa s). The lower viscosity memory 'forgets' the late-Pleistocene and early-Holocene glacial change, and is increasingly sensitive to the past millennium as the viscosity decreases to values typical of the asthenosphere immediately below tectonically active regions ($\eta < 5 \times 10^{19}$ Pa s). Stratification of the mantle alters the predicted pattern of uplift, but does not substantially affect the sensitivity to timing (Ivins & James 2004).

Beneath cratonic lithosphere, like the Canadian Shield, mantle viscosity may be anomalously high. Recent inversions of RSL and geodetic data by Wolf *et al.* (in press) indicate that 10^{21} and 10^{22} Pa s are possible upper bounds for the regional viscosity of the upper mantle and top of the lower mantle, respectively, beneath Hudson Bay. Global GIA-based estimates of volume averaged upper and lower mantle viscosity values are roughly 7 x 10^{20} and 2 x 10^{22}, respectively (Kaufmann & Lambeck 2002). On the other hand, a radial viscosity profile for the mantle may be determined by combining global GIA data with models derived from global gravity, seismic tomography and geodynamic data (Mitrovica & Forte 2004). The latter are likely representative of the globally averaged mantle. We do not know which mantle better characterizes the Antarctic sub-lithospheric environment, although it is probable that the upper mantle beneath West Antarctica has smaller viscosity values than beneath East Antarctica.

Computations of the crustal uplift (left frames) and time varying geoid (right frames) for models with a relatively 'average' (Fig. 6) and 'stiff' mantle profile (Fig. 7) reveal that the differences are small, but not altogether insignificant. The 'average' global mantle predicts larger amplitude present-day uplift and geoid changes. A subtle effect can be seen in the pattern of uplift predicted in the Ross Sea, just east of the Transantarctic Mountain Ranges, in comparing Figs 6 & 7. Neither the 'stiff' nor the 'average' mantle viscosity profiles 'forget' the ice load that existed near GLW (Hall *et al.* 2001, see Fig. 1) in the Ross Sea sector from LGM to early-Holocene time shown in Fig. 2. The difference is, however, measurable, and is important for uplift data obtained in the Transantarctic Mountain Ranges (e.g. Willis *et al.* 2003, Raymond *et al.* 2004).

The peak uplift values predicted in Figs 6 & 7 are about 12–18 mm yr^{-1} and 6–12 mm yr^{-1} for 'stiff' and 'average'

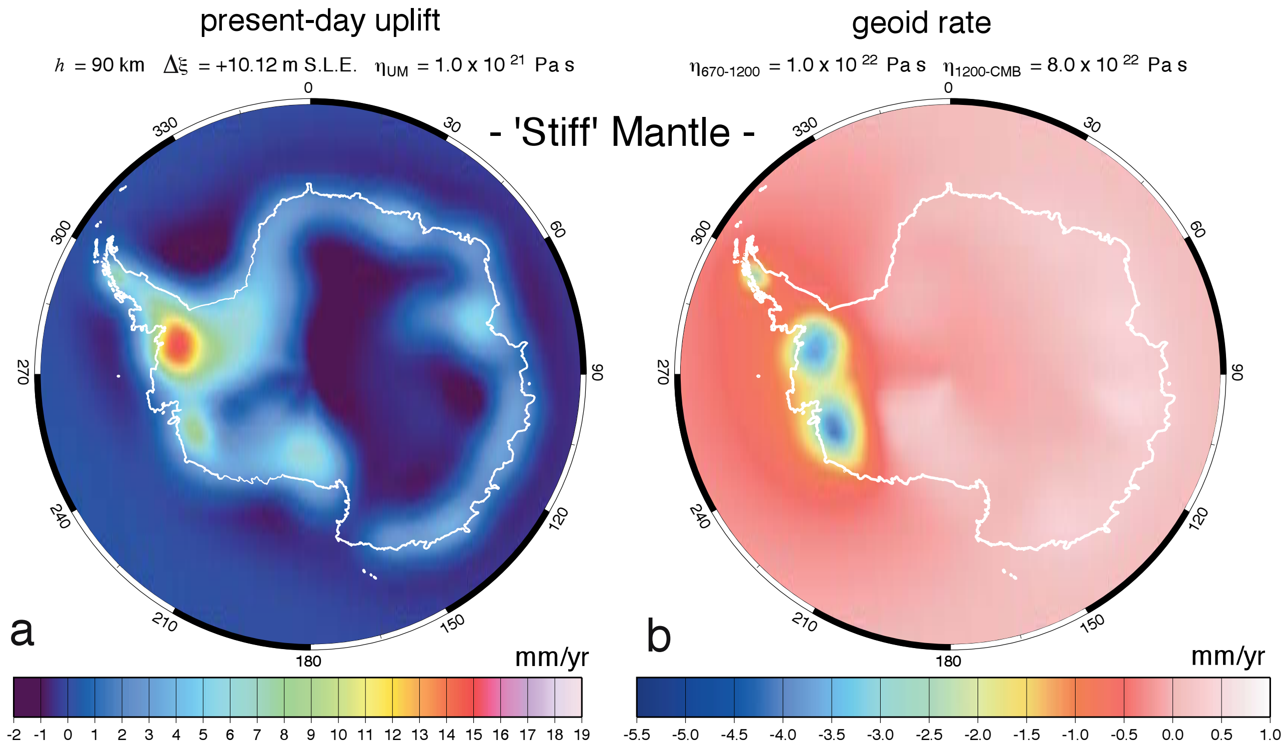

Fig. 7. Same as Fig. 6, but with higher viscosity in the upper mantle and top of the lower mantle, as indicated in the figure. This 'stiffer' mantle is near the upper bound that fits GIA crustal uplift data near Hudson Bay, Canada (Wolf *et al.* in press) and the global estimate of Mitrovica & Forte (2004).

mantle, respectively. The predictions in Figs 6 & 7 feature widespread subsidence across the East Antarctic Plateau at rates of 1–2 mm yr^{-1} primarily due to forebulge collapse. The subsidence will have to be accounted for when interpreting precise altimetric height data from the IceSat satellite (Wahr *et al.* 2000, Zwally *et al.* 2002) and follow-on missions. The predicted values of uplift and geoid rate for 'average' mantle are roughly comparable to the D91-1.5 model computed in Ivins *et al.* (2001) but are generally about a factor of 2 smaller than in Wahr *et al.* (2000) (fig. 3a, therein). The IJ05 model has ice change continuing to the present-day and this, presumably, causes the slight enhancement (~2 mm yr^{-1}) compared to D91-1.5. The latter model assumes larger total ESLR ($\Delta\xi$ ~ 12.5 m) but evolution terminates at 2 kyr BP.

Huybrechts & Le Meur (1999) computed bedrock uplift rates (h = 100 km, $\eta_{UM} = 5 \times 10^{20}$ Pa s, $\eta_{670\text{-}1200} = \eta_{1200\text{-CMB}} = 1 \times 10^{21}$ Pa s, $\Delta\xi$ ~ 12 m) with peak uplift rates exceeding 100 mm yr^{-1}. The difference is largely due to Huybrechts & Le Meur's (1999) larger Late Holocene ice mass change ($\Delta\xi \cong$ 3.3m ESLR since 3.2 kyr compared to IJ05 in which $\Delta\xi \cong$ 0.71m ESLR since ~3.2 kyr BP (see Fig. 3 and Table III). Nakada *et al.* (2000) found results similar to the uplift rates in Figs 6 & 7 (with peak values near 10 mm yr^{-1}) using a load model that initiated deglaciation at 12 kyr and terminated at 6 kyr.

Conclusions

Glacioisostatic research in Antarctica is unusual, compared to the Laurentide and Fennoscandian cases, for two reasons. First, there is a scarcity of near-field relative sea-level (RSL) records and, second, the dynamic Antarctic ice sheet has undergone substantial changes throughout the Holocene (Denton & Hughes 2002, Bindschadler & Bentley 2002, Ng & Conway 2004) and is changing rapidly at present (Bindschadler 2002, Thomas *et al.* 2004). In this paper we have reviewed information that contributes to building a new 21 kyr ice chronology ('IJ05'). The history predicts very different forward model predictions of vertical crustal velocities that depend critically on assumed mantle creep strength, or viscosity. The viscosity-dependence interacts strongly with the relatively recent (0–3 kyr BP) ice load history to determine predicted present-day rates. Future studies will rely on integrating space geodetic techniques (GRACE, GPS, CryoSat) with the small number of RSL curves that can be reconstructed for the near and intermediate field (Hall & Denton 1999, Nakada *et al.* 2000, Bentley *et al.* 2005). One theme of future research should be to provide control on regional mantle viscosity. Lack of constraint on this parameter is a major obstacle to improving GIA predictions for Antarctica.

Antarctic GIA has a substantial importance globally, not just for its contribution to late-Pleistocene and Holocene

ESLR, but also for its important role in the analysis of present-day low-wavelength gravity and sea-level change (Ivins *et al.* 1993, Mitrovica & Peltier 1993, James & Ivins 1997, Church *et al.* 2004). In addition, better GIA modelling in Antarctica will assist the analysis of GPS and VLBI (Very Long Baseline Interferometry) data to provide a more robust southern hemispheric realization of the International Terrestrial Reference Frame (ITRF). The new IJ05 model and crustal responses presented here promote the complementary goals of providing a stronger global geodetic framework and better understanding past and present Antarctic ice mass change and sub-Antarctic Earth rheology.

Acknowledgements

This work was performed at the Jet Propulsion Laboratory, Caltech, and at the Pacific Geoscience Centre, Geological Survey of Canada. NASA's GRACE Investigator Team and a grant from the Interdisciplinary Science Program in NASA's Science Mission Directorate supported this research. Support from the University of Victoria high-performance computing facility is gratefully acknowledged. We thank Michael Bentley, Bob Bindschadler, Andrea Donnellan, James Fastook, Carol Raymond, Eric Rignot, Ingo Sasgen, Mirko Scheinert, Isabella Velicogna, Ed Waddington, Mike Willis, Terry Wilson, Xiaoping Wu and Victor Zlotnicki for insightful discussion. Reviews by Masao Nakada, Georg Kaufmann and an anonymous reviewer were extremely helpful. Geological Survey of Canada contribution no. 2005127.

References

Ackert, R.P., Barclay, D.J., Borns, H.W., Calkin, P.E., Kurz, M.D., Fastook, J.L. & Steig. E.J. 1999. Measurements of past ice sheet elevations in interior West Antarctica. *Science*, **286**, 276–280.

Anderson, J.B. & Shipp, S.S. 2001. Evolution of the West Antarctic Ice Sheet. *Antarctic Research Series*, **77**, 45–57.

Anderson, J.B., Shipp, S.S., Lowe, A.L., Smith-Wellner, J. & Mosola, A.B. 2002. The Antarctic ice sheet during the Last Glacial Maximum and its subsequent retreat. *Quarternary Science Reviews*, **21**, 49–70.

Bentley, M.J. 1999. Volume of Antarctic ice at the Last Glacial Maximum, and its impact on global sea level change. *Quaternary Science Reviews*, **18**, 1569–1595.

Bentley, M.J., Hodgson, D.A., Smith, J.A. & Cox, N.J. 2005. Relative sea level curves for the South Shetland Islands and Marguerite Bay, Antarctic Peninsula. *Quaternary Science Reviews*, **24**, 1203–1216.

Bentley, M.J. & Anderson, J.B. 1998. Glacial and marine geological evidence for the ice sheet configuration in the Weddell Sea–Antarctic Peninsula region during the Last Glacial Maximum. *Antarctic Science*, **10**, 309–325.

Bindschadler, R. & Bentley, C.R. 2002. On thin ice? *Scientific American*, **287**, 98–105.

Bindschadler, R. 2002. History of lower Pine Island Glacier, West Antarctica. *Journal of Glaciology*, **48**, 536–544.

Canals, M., Urgeles, R. & Calafat, A.M. 2000. Deep sea-floor evidence of past ice streams. *Geology*, **28**, 31–34.

Church, J.A., White, N.J., Coleman, R., Lambeck, K. & Mitrovica, J.X. 2004. Estimates of the regional distribution of sea level rise over the 1950–2000 period. *Journal of Climate*, **17**, 2609–2625.

Conway, H., Hall, B.L., Denton, G.H., Gades, A.M. & Waddington, E.D. 1999. Past and future grounding-line retreat of the West Antarctic ice sheet. *Science*, **286**, 280–283.

Cowdery, S., Stone, J., Balco, G., Finkel, R.C. & Sugden, D. 2004. Glacial history of Marie Byrd Land – from thousands to millions of years. *11th Annual WAIS Workshop, Sept. 29–Oct. 2, 2004, Algonkian Park*, abstract. http//:igloo.gsfc.nasa.gov/wais/pastmeetings/abstracts04/Cowdery.htm.

Denton, G.H., Prentice, M.L. & Burkle, L.H., 1991. Cainozoic history of the Antarctic ice sheet. *In* Tingey, R.J., *ed. The geology of Antarctica*. Oxford: Clarendon Press, 365–433.

Denton, G.H., Bockheim, J.G., Rutford, R.H. & Andersen, B.G. 1992. Glacial history of the Ellsworth Mountains, West Antarctica. *Geological Society of America Memoir*, **170**, 403–432.

Denton, G.H. & Hughes, T. 1981. *The last great ice sheets*. New York: Wiley-Interscience, 484 pp.

Denton, G.H. & Hughes T.J. 2002. Reconstructing the Antarctic ice sheet at the Last Glacial Maximum. *Quaternary Science Reviews*, **21**, 193–202.

Dietrich, R., Rülke, A., Ihde, J., Lindner, K., Miller, H., Niemeier, W., Schenke, H.-W. & Seeber, G. 2004. Plate kinematics and deformation status of the Antarctic Peninsula based on GPS. *Global and Planetary Change*, **42**, 313–321.

Domack, E.W., Jull, A.T.J. & Nakao, S. 1991. Advance of East Antarctic outlet glaciers during the Hypsithermal: implications for the volume state of the Antarctic ice sheet under global warming. *Geology*, **19**, 1059–1062.

Donnellan, A. & Luyendyk, B.P. 2004. GPS evidence for a coherent Antarctic plate and for postglacial rebound in Marie Byrd Land. *Global and Planetary Change*, **42**, 305–311.

Emslie, S.D., Berkman, P.A., Ainley, D.G., Coats, L. & Polito, M. 2003. Late-Holocene initiation of ice-free ecosystems in the southern Ross Sea, Antarctica. *Marine Ecology Progress Series*, **262**, 19–25.

Evans, J., Dowdeswell, J.A. & O'Cofaigh, C. 2004. Late Quaternary submarine bedforms and ice sheet flow in Gerlache Strait and on the adjacent continental shelf, Antarctic Peninsula. *Journal of Quaternary Science*, **19**, 397–407.

Fleming, K., Johnston, P., Zwartz, D., Yokoyama, Y., Lambeck, K. & Chappell, J. 1998. Refining the eustatic sea-level curve since the Last Glacial Maximum using far- and intermediate-field sites. *Earth and Planetary Science Letters*, **163**, 327–342.

Fogwill, C.J., Bentley, M.J., Sugden, D.E., Kerr, A.R. & Kubik, P.W. 2004. Cosmogenic nuclides ^{10}Be and ^{26}Al imply limited Antarctic ice sheet thickening and low erosion in the Shackleton Range for > 1 m.y. *Geology*, **32**, 265–268.

Fox Maule, C., Purucker, M.E., Olsen, N. & Mosegaard, K. 2005. Heat flux anomalies in Antarctica revealed by satellite magnetic data. *Science*, **309**, 464–467.

Gore, D.B., Rhodes, E.J., Augustinus, P.C., Leishman, M.R., Colhoun, E.A. & Rees-Jones, J. 2001. Bunger Hills, East Antarctica: ice free at the Last Glacial Maximum. *Geology*, **29**, 1103–1106.

Hall, B.L. & Denton, G.H. 1999. New relative sea-level curves for the southern Scott Coast, Antarctica: evidence for Holocene deglaciation of the western Ross Sea. *Journal of Quaternary Science*, **14**, 641–650.

Hall, B.L., Denton, G.H. & Overturf, B. 2001. Glacial Lake Wright, a high level Antarctic lake during the LGM and early Holocene. *Antarctic Science*, **13**, 53–60.

Hall, B.L., Baroni, C. & Denton, G.H. 2004. Holocene relative sea-level history of the southern Victoria Land Coast, Antarctica. *Global and Planetary Change*, **42**, 241–263.

HILLENBRAND, C.-D., BAESLER, A. & GROBE, A.H. 2005. The sedimentary record of the last glaciation in the western Bellingshausen Sea (West Antarctia): implications for the interpretation of diamictons in a polar-marine setting. *Marine Geology*, **216**, 191–204.

HJORT, C., INGÓLFSSON, Ó., MÖLLER, P. & LIRIO, J.M. 1997. Holocene glacial history and sea-level changes on James Ross Island, Antarctic Peninsula, *Journal of Quaternary Science*, **12**, 259–273.

HOTHEM, L., MULLINS, J., GLOVER, R., WHILLANS, I., WILSON, T. & WILLIS, M. 2001. Transantarctic Mountains deformation monitoring network (TAMDEF) South Victoria Land - initial results. *SCAR Working Group on Geodesy and Geographic Information Report of the Second SCAR Antarctic Geodesy Symposium*, *Polish Academy of Sciences*, *Warsaw*, *14–16 July*, *1999*, SCAR Report No. 20. http://www.scar.org/publications/reports/20/Rep20d.html#TAMDEF

HUYBRECHTS, P. & LE MEUR E. 1999. Predicted present-day evolution patterns of ice thickness and bedrock elevation over Greenland and Antarctica. *Polar Research*, **18**, 299–308.

HUYBRECHTS, P. 2002. Sea-level changes at the LGM from ice-dynamic reconstructions of the Greenland and Antarctic ice sheets during the glacial cycles. *Quaternary Science Reviews*, **21**, 203–231.

HUYBRECHTS, P. 2004. Antarctica: modelling. *In* BAMBER, J.L. & PAYNE, A.J., *eds*. *Mass balance of the cryosphere: observations and modelling of contemporary and future changes*. Cambridge: Cambridge University Press, 491–523.

INGÓLFSSON, Ó. & HJORT, C. 1999. The Antarctic contribution to Holocene global sea level. *Polar Research,* **18**, 323–330.

INGÓLFSSON, Ó., HJORT, C. & HUMLUM, O. 2003. Glacial and climate history of the Antarctic Peninsula since the Last Glacial Maximum. *Arctic*, *Antarctic & Alpine Research*, **35**, 175–186.

IVINS, E.R. & JAMES, T.S. 2004. Bedrock response to Llanquihue Holocene and present-day glaciation in southernmost South America. *Geophysical Research Letters*, **31**, doi:10.1029/2004GL02150.

IVINS, E.R., SAMMIS, C.G. & YODER, C.F. 1993. Deep mantle viscous structure with prior estimate and satellite constraint. *Journal of Geophysical Research*, **98**, 4579–4609.

IVINS, E.R., RAYMOND, C.A. & JAMES, T.S. 2000. The influence of 5000 year-old and younger glacial mass variability on the present-day crustal rebound in the Antarctic Peninsula. *Earth*, *Planets and Space*, **52**, 1023–1029.

IVINS, E.R., RAYMOND, C.A. & JAMES, T.S. 2002. Late-Pleistocene, Holocene and present-day ice load evolution in the Antarctic Peninsula: models and predicted vertical crustal motion. *In* MITROVICA, J.X. & VERMEERSEN, B., *eds*. *Ice sheets*, *sea level and the dynamic Earth*, Geodynamics Series 29. Washington, DC: American Geophysical Union, 133–155.

IVINS, E.R., JAMES, T.S. & KLEMANN, V. 2003. Stress shadowing by the Antarctic ice sheet. *Journal of Geophysical Research*, **108**, doi: 10.1029/2002JB002182.

IVINS, E.R., WU, X., RAYMOND, C.A., YODER, C.F. & JAMES, T.S. 2001. Temporal geoid of a rebounding Antarctica and potential measurement by the GRACE and GOCE satellites. *In* SIDERIS, M., *ed*. *Gravity*, *geoid and geodynamics 2000*, *IAG Symposia*, *Vol. 123*. Heidelberg: Springer, 361–366.

JAMES, T.S. & IVINS, E.R. 1997. Global geodetic signatures of the Antarctic ice sheet. *Journal of Geophysical Research*, **102**, 605–633.

JAMES, T.S. & IVINS, E.R. 1998. Predictions of Antarctic crustal motions driven by present-day ice sheet evolution and by isostatic memory of the Last Glacial Maximum. *Journal of Geophysical Research*, **103**, 4993–5017.

KAUFMANN, G. 2000. Ice-ocean mass balance during the Late-Pleistocene glacial cycles in view of CHAMP and GRACE satellite missions. *Geophysical Journal International*, **143**, 142–156.

KAUFMANN, G. & LAMBECK, K. 2002. Glacial isostatic adjustment and radial viscosity profile from inverse modeling. *Journal of Geophysical Research*, **107**, doi: 10.1029/2001JB000941.

KAUFMANN, G., WU, P. & IVINS, E.R. 2005. Lateral viscosity variations beneath Antarctica and their implications on regional rebound motions and seismotectonics. *Journal of Geodynamics*, **39**, 165–181.

LAMBECK, K., ANZIDEI, M., ANTONIOLI, F., BENINI, A. & ESPOSITO, A. 2004. Sea level in Roman time in the central Mediterranean and implications for recent change. *Earth and Planetary Science Letters*, **224**, 563–575.

LICHT, K.J., JENNINGS, A.E., ANDREWS, J.T. & WILLIAMS, K.M. 1996. Chronology of late Wisconsin ice retreat from the western Ross Sea, Antarctica. *Geology*, **24**, 223–226.

LICHT, K.J. 2004. The Ross Sea's contribution to eustatic sea-level during meltwater pulse 1A. *Sedimentary Geology*, **165**, 343–353.

LORIUS, C., J. JOUZEL, C. RITZ, L. MERLIVAT, N.I. BARKOV, Y.S. KOROTKEVICH & KOTLYAKOV, V.M. 1985. A 150 000-year climate record from Antarctic ice. *Nature*, **316**, 591–596.

LOWE, A.L. & ANDERSON, J.B. 2002. Reconstruction of the West Antarctic Ice Sheet in Pine Island Bay during the last glacial maximum and its subsequent retreat history. *Quaternary Science Reviews*, **21**, 1879–1897.

MORELLI, A. & DANESI, S. 2004. Seismological imaging of the Antarctic continental lithosphere: a review. *Global and Planetary Change*, **42**, 155–165.

MIURA, H., MORIWAKI, K., MAEMOKU, H. & HIRAKAWA, K. 1998. Fluctuations of the Antarctic ice sheet margin since the last glaciation from stratigraphy of raised beach deposits along the Syoa Coast. *Annals of Glaciology*, **27**, 297–301.

MITROVICA, J.X. & PELTIER,W.R. 1993. Present-day secular variations in the zonal harmonics of Earth's geopotential. *Journal of Geophysical Research*, **98**, 4509–4526.

MITROVICA, J.X. & FORTE, A.M. 2004. A new inference of mantle viscosity based upon joint inversion of convection and glacial isostatic adjustment data. *Earth and Planetary Science Letters*, **225**, 177–189.

NAKADA, M., & LAMBECK, K. 1988. The melting history of the late Pleistocene Antarctic ice sheet. *Nature*, **333**, 36–40.

NAKADA, M. & LAMBECK, K. 1989. Late Pleistocene and Holocene sea-level change in the Australian region and mantle rheology. *Geophysical Journal International*, **96**, 497 –517.

NAKADA, M., KIMURA, R., OKUNO, J., MORIWAKI, K., MIURA, H. & MAEMOKU, H. 2000. Late Pleistocene and Holocene melting history of the Antarctic ice sheet derived from sea level variations. *Marine Geology*, **167**, 85–103.

NEGUSINI, M. MANCINI, F. GANDOLFI, S. & CAPRA, A. 2005. Terra Nova Bay GPS permanent station (Antarctica): data quality and first attempt in the evaluation of regional displacement. *Journal of Geodynamics*, **39**, 81–90.

NG, F. & CONWAY, H. 2004. Fast-flow signature in the stagnated Kamb Ice Stream, West Antarctica. *Geology*, **32**, 481–484.

OBERHOLZER, P., BARONI, C., SCHAEFER, J.M., OROMBELLI, G., IVY-OCHS, S., KUBIK, P.W., BAUR, H. & WIELER, R. 2003. Limited Pliocene/Pleistocene glaciation in Deep Freeze Range, northern Victoria Land, Antarctica, derived from *in situ* cosmogenic nuclides. *Antarctic Science*, **15**, 493–502.

PATTYN, F. & DECLEIR, H. 1998. Ice dynamics near Antarctic marginal mountain ranges: implications for interpreting the glacial-geological evidence. *Annals of Glaciology*, **27**, 329–332.

PARRENIN, F., RÉMY, F., RITZ, C., SIEGERT, M. J. & JOUZEL, J. 2004. New modelling of the Vostok ice flow line and implication for the glaciological chronology of the Vostok ice core. *Journal of Geophysical Research*, **109**, doi: 10.1029/2004JD004561.

PAYNE, A.J., SUGDEN, D.E. & CLAPPERTON, C.M. 1989. Modeling the growth and decay of the Antarctic Peninsula ice sheet. *Quaternary Research*, **31**, 119–134.

PELTIER, W.R. 2004. Global glacial isostasy and the surface of the ice-age Earth: the ICE-5G (VM2) model and GRACE. *Annual Review of Earth and Planetary Sciences,* **32**, 111–149.

Raymond, C.A., Ivins, E.R., Heflin, M.B. & James, T.S. 2004. Quasi-continuous Global Positioning System measurements of glacial isostatic adjustment in the Northern Transantarctic Mountains. *Global and Planetary Change*, **42**, 295–303.

Rignot, E. & Thomas, R.H. 2002. Mass balance of polar ice sheets. *Science*, **297**, 1502–1506.

Rignot, E., Casassa, G., Krabill, W., Goginen, P., Rivera, A. & Thomas, R. 2004a. Accelerated ice discharge from the Antarctic Peninsula following the collapse of Larsen B ice shelf. *Geophysical Research Letters*, **31**. doi: 10.1029/2004GL020697.

Rignot, E., Thomas, R., Casassa, G., Frederick, E., Gogineni, S., Kanagaratnam, P., Krabill, W., Rivera, A., Russell, R., Sonntag, J., Swift, R., Teitel, C. & Yungel, J. 2004b. Revised estimate of the mass balance of the glaciers draining into the Amundsen Sea sector of West Antarctica using data from the 2002 NASA/CECS airborne campaign. *Annals of Glaciology*, **39**, 231–237.

Scheinert, M., Ivins, E.R., Dietrich, R. & Rülke, A. 2005. Vertical crustal deformations in Dronning Maud Land, Antarctica: observations versus model predictions. *Antarctic Contributions to Global Earth Science*, *Proceedings IX ISAES*, *Potsdam*, *Sept. 1–6*, *2003*, in press.

Shipp, S., Anderson, J. & Domack, E. 1999. Late Pleistocene–Holocene retreat of the West Antarctic Ice Sheet system in the Ross Sea: Part 1 – geophysical results. *Geological Society of America Bulletin*, **111**, 1486–1516.

Steig, E.J., Fastook, J.L., Zweck, C., Goodwin, I.D., Licht, K.J., White, J.W.C. & Ackert, R.P. 2001. West Antarctic ice sheet elevation changes. *Antarctic Research Series*, **77**, 75–90.

Stone, J.O., Balco, G.A., Sugden, D.E., Caffee, M.W., Sass, L.C., Cowdery, S.G. & Siddoway, C. 2003. Holocene deglaciation of Marie Byrd Land, West Antarctica. *Science*, **299**, 99–102.

Takada, M., Tani, A., Miura, H., Moriwaki, K. & Nagatomo T. 2003. ESR dating of fossil shells in the Lützow–Holm Bay region, East Antarctica. *Quaternary Science Reviews*, **22**, 1323–1328.

Thomas, R., Rignot, E., Casassa, G., Kanagaratnam, P., Acuna, C., Akins, T., Brecher, H., Frederick, E., Gogineni, P., Krabill, W., Manizade, S., Ramamoorthy, H., Rivera, A., Russell, R., Sonntag, J., Swift, R., Yungel, J. & Zwally, J. 2004. Accelerated sea-level rise from West Antarctica. *Science*, **306**, 255–258.

Todd, C., Stone, J. & Mann, D. 2004. Deglaciation of the southern Ellsworth Mountains, Weddell Sea Sector of the West Antarctic Ice Sheet. *11th Annual WAIS Workshop, Sept. 29–Oct. 2, 2004, Algonkian Park*, abstract. http//:igloo.gsfc.nasa.gov/wais/pastmeetings/abstracts04/Todd_Stone.htm

Tosi, N., Sabadini, R., Marotta, A.M. & Vermeersen, L.L.A. 2005. Simultaneous inversion of the Earth's mantle viscosity and ice mass balance in Antarctica and Greenland. *Journal of Geophysical Research*, **110**, doi: 10.1029/2004JB003236.

Toracinta, R.E., Oglesby, R.J. & Bromwich, D.H. 2004. Atmospheric. Response to Modified CLIMAP ocean boundary conditions during the Last Glacial Maximum. *Journal of Climate*, **17**, 504–522.

Tushingham, A.M. & Peltier, W.R. 1991. ICE-3G: A new global model of late Pleistocene deglaciation based upon geophysical predictions of post glacial relative sea level change. *Journal of Geophysical Research*, **96**, 4497–4523.

van Ommen, T.D., Morgan, V. & Curran, M.A.J. 2004. Deglacial and Holocene changes in accumulation at Law Dome. *Annals of Glaciology*, **39**, 359–365.

Verleyen, E., Hodgson, D.A., Sabbe, K. & Vyverman, W. 2004. Quaternary deglaciation and climate history of the Larsemann Hills (East Antarctica). *Journal of Quaternary Science*, **19**, 361–375.

Verleyen, E., Hodgson, D.A., Milne, G.A., Sabbe, K. & Vyverman, W. 2005. Relative sea-level history from the Lambert Glacier region, East Antarctica, and its relation to deglaciation and Holocene glacier readvance. *Quaternary Research*, **63**, 45–52.

Waddington, E.D., Conway, H., Steig, E.J., Alley, R.B., Brook, E.J., Taylor, K. & White, J.W.C. 2005. Decoding the dipstick: thickness of Siple Dome, West Antarctica, at the Last Glacial Maximum. *Geology*, **33**, 281–284.

Wahr, J., Wingham, M.D. & Bentley, C. 2000. A method of combining IceSat and GRACE satellite data to constrain Antarctic mass balance. *Journal of Geophysical Research*, **105**, 16279–16294.

Willis, M., James, T. & Wilson, T. 2003. Horizontal crustal motions in the Antarctic interior: comparison of GPS measurements and post-glacial rebound model predictions. *EGS–AGU–EUG Joint Assembly*, *Nice*, *France*, *6–11 April 2003*, abstract #2988. available at http://www.cosis.net/abstracts/EAE03/02988/EAE03-J-02988.pdf

Watanabe, O., Jouzel, J., Johnsen, S., Parrenin, F., Shoji, H. & Yoshida, N. 2003. Homogeneous climate variability across East Antarctica over the past three glacial cycles. *Nature*, **422**, 509–512.

Wolf, D., Klemann, V., Wunsch, J. & Zhang, F. In press. A reanalysis and reinterpretation of geodetic and geological evidence of glacial-isostatic adjustment in the Churchill region, Hudson Bay. *Surveys in Geophysics*.

Wu, X., M. Watkins, E.R. Ivins, P. Wang, R. Kwok & J. Wahr 2002. Toward global inverse solutions for the determination of current and past ice mass variations: Contribution of secular satellite gravity and topography change measurements. *Journal Geophysical Research*, **107**, doi: 10.1029/201JB000543.

Zwally, H.J., Schutz, B., Abdalati, W. & 13 others. 2002. ICESat's laser measurements of polar ice, atmosphere, ocean and land. *Journal of Geodynamics*, **34**, 405–445.

Zwartz, D., Bird, M., Stone, J. & Lambeck, K. 1998. Holocene sea-level change and ice sheet history in the Vestfold Hills, East Antarctica. *Earth and Planetary Science Letters*, **155**, 131–145.